Available online at www.sciencedirect.com
ScienceDirect
European Journal of Medicinal Chemistry 43 (2008) 2103–2115
EUROPEAN JOURNAL OF MEDICINAL CHEMISTRY
http://www.elsevier.com/locate/ejmech

Original article

Synthesis, screening for antitubercular activity and 3D-QSAR studies of substituted *N*-phenyl-6-methyl-2-oxo-4-phenyl-1,2,3,4-tetrahydro-pyrimidine-5-carboxamides

Vijay Virsodia [a], Raghuvir R.S. Pissurlenkar [b], Dinesh Manvar [c], Chintan Dholakia [d], Priti Adlakha [e], Anamik Shah [a,*], Evans C. Coutinho [b,**]

[a] *Department of Chemistry, Saurashtra University, Rajkot 360 005, Gujarat, India*
[b] *Department of Pharmaceutical Chemistry, Bombay College of Pharmacy, Kalina, Santacruz (E), Mumbai 400 098, Maharashtra, India*
[c] *Calyx Chemicals and Pharmaceuticals Ltd., Mumbai 400 072, Maharashtra, India*
[d] *Unimark Remedies Ltd., Bavla, Ahemdabad 382 220, Gujarat, India*
[e] *Institute of Applied Synthetic Chemistry, Vienna University of Technology, Vienna, Austria*

Received 29 May 2007; received in revised form 26 June 2007; accepted 20 August 2007
Available online 11 September 2007

Abstract

Multi-drug resistance to commonly used antitubercular drugs has propelled the development of new structural classes of antitubercular agents. This paper reports the synthesis, evaluation and 3D-QSAR analysis of a set of substituted *N*-phenyl-6-methyl-2-oxo-4-phenyl-1,2,3,4-tetrahydropyrimidine-5-carboxamides as antitubercular agents. Substituted acetoacetanilides were reacted with various aromatic aldehydes and urea which yielded the tetrahydropyrimidine derivatives with a phenyl carbamoyl group at C_5 position, and with various substitutions on the 4-phenyl and the *N*-phenyl aromatic rings. All compounds were screened for antitubercular activity against *Mycobacterium tuberculosis* H_{37}Rv strain. The QSAR models were generated on a training set of 23 molecules. The molecules were aligned using the atom-fit and field-fit techniques. The CoMFA and CoMSIA models generated on the molecules aligned by the atom-fit method show a correlation coefficient (r^2) of 0.98 and 0.95 with cross-validated r^2(q^2) of 0.68 and 0.58, respectively. The 3D-QSAR models were externally validated against a test set of 7 molecules for which the predictive r^2 (r^2_{pred}) is recorded as 0.41 and 0.32 for the CoMFA and CoMSIA models, respectively. The CoMFA and CoMSIA contours helped to design some new molecules with improved activity.

Keywords: Tetrahydropyrimidines; Antitubercular activity; CoMFA; CoMSIA

1. Introduction

One-third of the world's population is infected with *Mycobacterium tuberculosis* which is the leading cause of death [1,2] in the developing world. Approximately 2 million people die every year [3].

Multi-drug resistance tuberculosis (MDR-TB), defined as resistance to at least isoniazid and rifampicin [4], is a serious threat to tuberculosis control and prevention. Isoniazid blocks the biosynthesis of mycolic acids, essential components of mycobacterial cell wall, and is believed to be oxidized by catalase peroxidase (*Kat*G) to the active form [5]. Mutations in the *Kat*G and the *Inh*A genes are associated with 70–80% of INH resistant *M. tuberculosis* isolates [6]. Resistance to rifampicin has been associated with mutations in the 81-bp core region of the *rpo*B gene encoding the β-subunit of RNA polymerase [7,8], in over 90% cases. The development of resistance by *M. tuberculosis* to commonly used antitubercular

* Corresponding author. Tel.: +91 281 2581013; fax: +91 281 2576802.
** Corresponding author. Tel.: +91 22 2667 0871; fax: +91 22 2667 0816.
E-mail addresses: anamik_shah@hotmail.com (A. Shah), evans@bcpindia.org (E.C. Coutinho).

0223-5234/$ - see front matter © 2007 Elsevier Masson SAS. All rights reserved.
doi:10.1016/j.ejmech.2007.08.004

drugs necessitates a longer duration of therapy. The emergence of multi-drug resistance has forced the development of new structural classes of antitubercular agents, with several of them showing promising activity against *M. tuberculosis* [9].

There are several reports in the literature of new structural classes of antitubercular agents. Derivatives of imidazoles have MIC values between 0.015 and 0.25 μg/mL against various drug-resistant strains of *M. tuberculosis*, and are highly active both *in vitro* and *in vivo* [10,11]. Acyclic deoxy monosaccharide derivatives, from the carbohydrate class, have MIC value of 3.125 μg/mL against $H_{37}Rv$ strain [12]. The most effective derivative from the benzoic acid hydrazone class with a MIC of 2.0 μg/mL is a good lead for further drug design studies [13]. Calanolide A, a naturally occurring coumarin derivative and an inhibitor of HIV-1 reverse transcriptase also shows promising *in vitro* activity against *M. tuberculosis* with MIC value of 3.13 μg/mL [14,15]. The purine derivatives are quite potent against *M. tuberculosis* $H_{37}Rv$ strain with MIC of 0.78 μg/mL [16,17]. The most effective compounds of the pyrrole class exhibit MIC values of 0.4 μg/mL and 0.7 μg/mL against *Mycobacterium avium* and *M. tuberculosis*, respectively [18,19]. MIC value of 0.5 mcmol/L has been reported for benzoxazine derivatives, against *M. tuberculosis* [20]. Various diterpenoids derived from plants have been described to possess tuberculosis activity against *M. tuberculosis* [21,22]. These new structural classes build important plots for the focused development of new antitubercular drugs.

Pyridines and pyrimidines have also been identified with antitubercular activity and can be developed as new structural classes of antitubercular agents. Amongst the pyridines, *N*-alkyl-1,2-dihydro-2-thioxo-3-pyridine carbothioamides have been recognized as a novel class of compounds with good antitubercular activity. Two compounds in this series have an MIC of 0.50 μg/mL [23]. *N*-Pyridinylsalicylamides which also belong to the pyridine class of compounds have an MIC of 2.0 μg/mL. The effect of various substitutions on activity of this class was studied by QSAR [24]. Within the pyrimidine group, 2,4-diaminopyrimidines have been identified with IC_{50} of 0.0058 μM and a safety index >600 [25]. The most effective derivative in the chloropyrimidine series has an MIC of 0.78 μg/mL [26], while the most successful compound from the anilinopyrimidine series displays an MIC of 3.12 μg/mL [27]. Thymidine monophosphate derivatives have been evaluated for binding to thymidine monophosphate kinase of *M. tuberculosis*. The most effective inhibitor has a K_i of 10.5 μM [28]. Thus, this structural class holds great hope for development of new and effective antitubercular agents.

We had synthesized and evaluated several 1,4-dihydropyridines bearing a lipophilic group, as antitubercular agents, on the assumption that these compounds could act as prodrugs, which after penetration would be converted to the 3,5-carboxylate anions by enzymatic hydrolysis. The most effective analogs show more than 97% inhibition of mycobacterium at a concentration of 2.50 μg/mL, and this series was examined in detail by QSAR analysis [29,30]. In continuation of this work, we sought to explore and modify the 1,4-dihydropyridines to tetrahydropyrimidines (which can be viewed as aza analogs of pyridines) for development of new antitubercular agents and to subject them to a QSAR analysis to understand the relationships between structure and activity for this class. This paper describes the synthesis, evaluation and 3D-QSAR studies of a series of *N*-phenyl-6-methyl-2-oxo-4-phenyl-1,2,3,4-tetrahydro-pyrimidine-5-carboxamides.

2. Results and discussion

2.1. Chemistry

Various substituted acetoacetanilides (**2a–n**) were prepared by reacting substituted amines and ethyl acetoacetate in toluene with a catalytic amount of NaOH or KOH (Scheme 1). The reaction mixture was heated at 120 °C for 10–15 h. Fourteen different acetoacetanilides were synthesized bearing various electron donating and electron withdrawing groups like 2,3-diCH_3; 3,4-diCH_3; 4-CH_3; H; 2,5-diCH_3; 2,4-diCH_3; 3-Cl-4-F; 4-F; 4-Cl; 2-Cl; 2-F; 4-OCH_3; 2,5-diCl and 3-NO_2 on the phenyl ring. Acetoacetanilides, thus obtained, were used as 1,3-diketone adducts for the multi-component Biginelli reaction.

The acetoacetanilides (**2a–n**) were reacted with substituted aldehydes and urea in methanol using conc. HCl in catalytic amount to obtain the title compounds (**3a–v**, **4a–g**) depicted in Scheme 2. The reaction time was found to vary from 5 to 10 h depending upon the substitutions on the aldehydes and the 1,3-diketones.

The structures of the synthesized compounds were confirmed by spectral analysis. The carbonyl group of NH–CO (amide) was observed at 1650–1690 cm^{-1} and the cyclic ketone was observed at 1700–1720 cm^{-1} in the IR spectra. In the NMR spectra, the proton attached to C_4 was observed between δ 4.2 and 6.0 ppm. The protons attached to the methyl group on C_6 are deshielded and were observed at δ 1.8–3.8 ppm. The signals of N_1H, N_3H and the NH of the carbamoyl group were observed downfield ($\delta = 7.2$–10.0 ppm). The molecular ion peaks (M^+) were in total agreement with the molecular weight. The elemental analysis was found to match the calculated elemental composition within the permissible error limits.

2.2. Antitubercular activity

Synthesized compounds (**3a–v**, **4a–g**) were tested for their antitubercular activity against *M. tuberculosis* $H_{37}Rv$ strain. Percentage inhibition data of compounds (**3a–v**, **4a–g**) are reported in Tables 1 and 2. Compounds **3c** and **4f**, with 2,3-dimethylphenyl and 3,4-dimethyl carbamoyl side chain, respectively, showed 65% and 63% inhibition. Thus, methyl group at these positions showed higher potency. But substitutions on 4-phenyl ring also alter the activity of compound. Compound **3m** is having 3,4-dimethylphenyl carbamoyl side chain as in compound **4f**, but NO_2 group is at *meta* position in compound **3c** and at *para* position in compound **3m** which

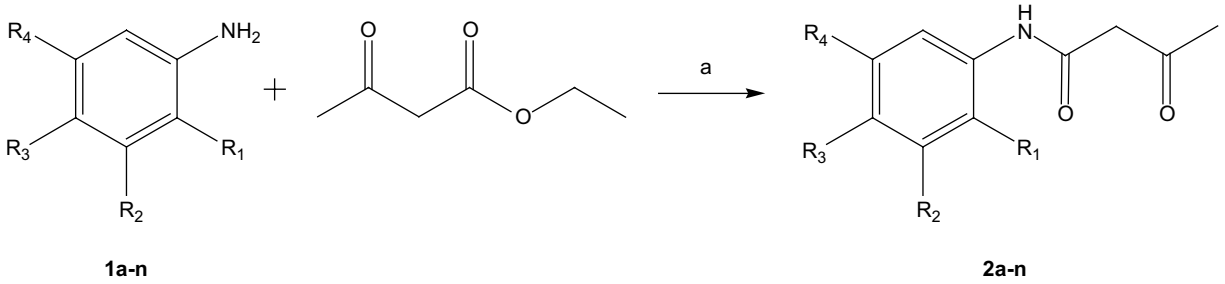

1a-n **2a-n**

Scheme 1. Reagents and conditions: (a) NaOH/KOH, toluene, 110 °C, 10–15 h.

leads to decrease in % inhibition from 63% to 13%. Thus, compound with methyl substitution on phenyl carbamoyl side chain with –OPh or $-NO_2$ substitution at *meta* position of 4-phenyl ring were more potent than same substitution on *para* position. The replacement of methyl groups in phenyl ring of phenyl carbamoyl side chain with halogen result in loss of potency. Compounds with halogen substituted at different position of phenyl ring of phenyl carbamoyl side chain do not showed good potency either with *meta* or *para* substituted 4-phenyl ring. Thus, it can be concluded that methyl groups on phenyl ring of C5 side chain with *meta* substituted 4-phenyl ring showed good potency. To find out structural requirement and better activity data, the results obtained were subjected to 3D-QSAR analysis.

2.3. QSAR study

2.3.1. Computational details

The 3D-QSAR techniques of CoMFA and CoMSIA were carried out with *Sybyl 7.1* (Tripos Inc., USA) [31] running on a Pentium IV computer under the Red Hat Linux Enterprise WS4.

2.3.2. Ligand preparation

The dataset was divided into a training set (23 molecules, Table 1) and a test set (7 molecules, Table 2) on the basis of chemical and biological diversity using the Tanimoto similarity coefficient [32].

For the QSAR study, the activity values were transformed as follows [33]:

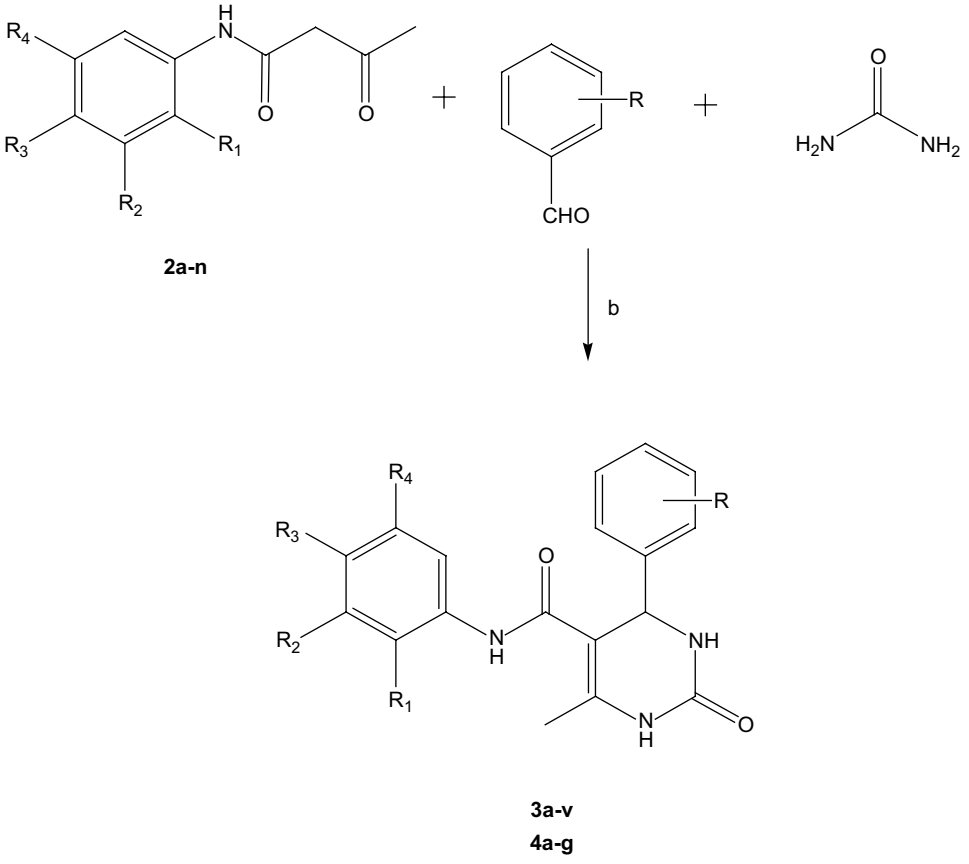

2a-n

3a-v

4a-g

Scheme 2. Reagents and conditions: (b) HCl, methanol, reflux, 5–10 h.

Table 1
Molecules used in the training set for CoMFA and CoMSIA studies

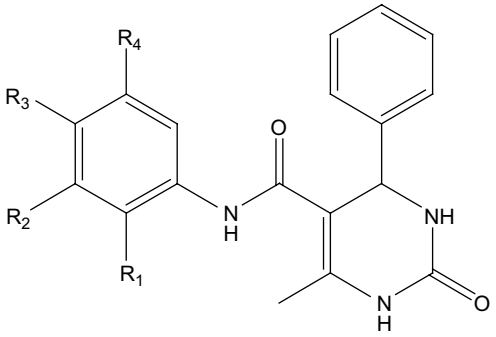

Compound	R	R_1	R_2	R_3	R_4	% Inhibition (μg/mL)	log activity[a]
3a	4-OCH_3	CH_3	H	H	CH_3	2	3.08
3b	3-OPh	CH_3	H	H	CH_3	27	4.40
3c	3-OPh	CH_3	CH_3	H	H	65	5.10
3d	2-NO_2	Cl	H	H	H	11	3.88
3e	4-NO_2	CH_3	H	H	CH_3	4	3.40
3f	4-Cl	H	H	H	H	6	3.54
3g	4-OH	F	H	H	H	18	4.08
3h	4-NO_2	Cl	H	H	Cl	18	3.14
3i	4-OH	CH_3	H	CH_3	H	12	3.88
3j	4-OH	H	NO_2	H	H	2	3.08
3k	3-Cl	H	Cl	F	H	48	4.77
3l	4-NO_2	F	H	H	H	4	3.39
3m	4-NO_2	H	CH_3	CH_3	H	13	3.96
3n	4-NO_2	CH_3	H	CH_3	H	12	3.92
3o	3-NO_2	Cl	H	H	H	26	4.34
3p	3-NO_2	H	Cl	F	H	29	4.42
3q	3-NO_2	F	H	H	H	24	4.27
3r	3-Cl	H	H	F	H	38	4.55
3s	4-NO_2	H	H	OCH_3	H	21	4.21
3t	3-NO_2	H	H	Cl	H	29	4.40
3u	3-NO_2	H	H	CH_3	H	28	4.36
3v	3-NO_2	H	H	F	H	30	4.40

MIC > 6.25 μg/mL.
[a] log acitivity calculated as described in text.

$$\log \text{activity} = -\log c + \text{logit}$$

where c is molar concentration = concentration (μg/mL) × 0.001/(molecular weight) and log it = log [% inhibition/(100−% inhibition)].

Table 2
Molecules used in the test set for CoMFA and CoMSIA studies

Compound	R	R_1	R_2	R_3	R_4	% Inhibition (μg/mL)	log activity[a]
4a	3-NO_2	CH_3	H	H	H	6	3.57
4b	4-Cl	Cl	H	H	H	26	4.33
4c	4-NO_2	H	H	Cl	H	9	3.79
4d	3-OPh	H	CH_3	CH_3	H	32	4.51
4e	4-NO_2	H	H	H	H	25	4.29
4f	3-NO_2	H	CH_3	CH_3	H	63	5.02
4g	4-NO_2	H	Cl	F	H	22	4.26

MIC > 6.25 μg/mL.
[a] log acitivity calculated as described in text.

The molecules were built using the *Builder* module in *Sybyl* 7.1. The crystal structure of methyl-4-(3-methoxyphenyl)-6-methyl-2-oxo-1,2,3,4-tetrahydropyrimidine-5-carboxylate [34] was used as the template (Fig. 1) to built the molecules in the dataset. The template structure has the pyrimidine ring in the boat conformation with the 4-phenyl ring in the axial orientation and the C_4 atom of the pyrimidine ring in an *S*-configuration. The ligand geometries were optimized by energy minimization with the Powel method using MMFF94 forcefield and charges for the atoms, till a gradient of 0.005 kcal/mol/Å was reached, maintaining the template structure rigid during the minimization.

2.3.3. Molecular alignment

The molecules of the dataset were aligned by two techniques. First by the atom-fit technique, using atoms common with the crystal structure of methyl-4-(3-methoxyphenyl)-6-methyl-2-oxo-1,2,3,4-tetrahydropyrimidine-5-carboxylate (Fig. 2a). In the second approach, the molecules were aligned by the field-fit technique where the steric and electrostatic fields of the most active molecule in the series were extracted and used for the alignment of the fields of the other molecules (Fig. 2b).

2.3.4. CoMFA and CoMSIA studies

CoMFA (Comparative Molecular Field Analysis) [35] and CoMSIA (Comparative Molecular Similarity Indices Analysis) [36–38] studies were carried out with the default settings for the 3D cubic lattice, the grid spacing, the probe atom, and the energy cutoff.

For CoMSIA, five physicochemical properties (steric, electrostatic, hydrophobic, and hydrogen-bond donor and acceptor) were explored, and the attenuation factor was set to the default value of 0.3. The CoMFA and CoMSIA descriptors were used as independent variables and the log activities as the dependent variable in a partial least squares (PLS) regression analysis [39] to derive the 3D-QSAR models. The models were internally evaluated by leave-one-out (LOO) cross-validation. The optimal number of components was determined by the SAMPLS [40] method which was subsequently used to derive the final QSAR models. In addition to the q^2, the conventional correlation coefficient r^2, and standard errors (SE) were also computed. The robustness of the models was gauged by cross-validation using leave-group-out (LGO) of 10 groups and bootstrapping [41] carried out with 100 runs. The CoMFA

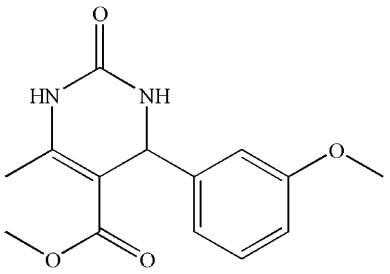

Fig. 1. Template structure for building the molecules in the training and test sets.

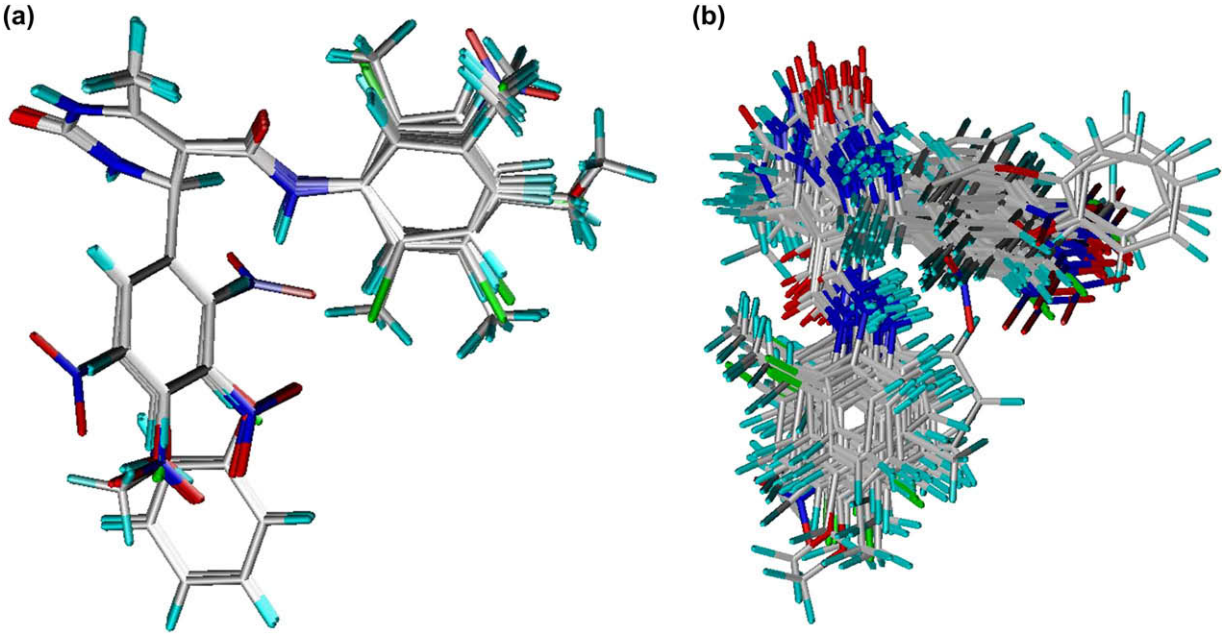

Fig. 2. (a) Atom-fit and (b) field-fit alignment for the dataset.

and CoMSIA models were also validated for their predictivity on an external dataset of 7 molecules. The statistical data are reported in Table 3.

The molecules that exhibited large residuals were reintroduced into the dataset with alternate conformations and the QSAR models regenerated. The statistical parameters – q^2 and r^2_{pred} of the CoMFA and CoMSIA models obtained by atom-fit alignment are better than the corresponding values for the models obtained by field-fit alignment (Table 3).

2.3.5. Graphical analysis

The CoMFA and CoMSIA contour maps were generated using scalar products of coefficients and standard deviation (STDEV × COEFF) set at 80% and 20% for favored and disfavored levels, respectively. The CoMFA and CoMSIA contours are depicted for the atom-fit alignment models in Figs. 3 and 4, respectively. The CoMFA model has equal steric and electrostatic contribution to the activity while electrostatic and hydrophobicity contributions are seen to dominate in the CoMSIA model.

Table 3
The statistics of the CoMFA and CoMSIA models

	Atom-fit alignment		Field-fit alignment	
	CoMFA	CoMSIA	CoMFA	CoMSIA
PLS statistics				
n	23	23	23	23
r^2	0.98	0.95	0.97	0.96
q^2 (LOO)	0.68	0.58	0.38	0.23
q^2 (LGO)	0.64	0.50	0.45	0.26
$r^2_{bootstrap}$	0.99	0.98	0.98	0.99
r^2_{pred}	0.41	0.32	0.60	0.36
F	184.85	45.85	234.60	70.78
SE	0.08	0.15	0.10	0.13
PLS components	6	6	3	6
Field contribution				
Steric	0.49	0.13	0.43	0.09
Electrostatic	0.51	0.31	0.57	0.34
Hydrophobic	–	0.33	–	0.25
Donor	–	0.08	–	0.16
Acceptor	–	0.15	–	0.16

The 3D-QSAR contours and their relation with the biological activity of molecules are described in Figs. 3–5. The CoMFA steric fields (green contours, Fig. 3a) favor substitution of bulky groups at the *meta* position of both the 5*N*-phenyl and the 4-phenyl moieties, while disfavored steric fields (yellow contours) are seen at the *para* position of the 4-phenyl group, which is also supported by the CoMSIA steric contours (Fig. 4a). In addition, disfavored steric CoMSIA contours are also seen at the *meta*′-position of the 5*N*-phenyl residue.

The CoMFA electrostatic contours depict that electropositive groups (blue contour, Fig. 3b) are favored at the *meta* position of the 5*N*-phenyl group and at the *ortho*′, *meta* and *para* positions of the 4-phenyl group. However, electronegative groups (red contour) at the *meta*′-position of the 4-phenyl moiety are likely to increase the activity. The CoMSIA electrostatic contours (Fig. 4b) also favor electropositive groups at the *para* and *ortho*′ positions of the 4-phenyl ring and in addition, electronegative groups at the *para* position of 5*N*-phenyl group. The hydrophobic contours of CoMSIA indicate desired and undesired hydrophobic regions around the two phenyl rings. The hydrophobic groups (white contours, Fig. 4c) would cause the activity to decrease when placed at the *meta*′ position of the 5*N*-phenyl ring or the *meta*′ and *para* positions of the 4-phenyl ring; small hydrophobic groups (yellow fields) are accepted at the *meta* position of the 5*N*-phenyl ring.

The H-bond donor fields are absent in the CoMSIA model. The disfavored fields of the H-bond acceptor are seen as red

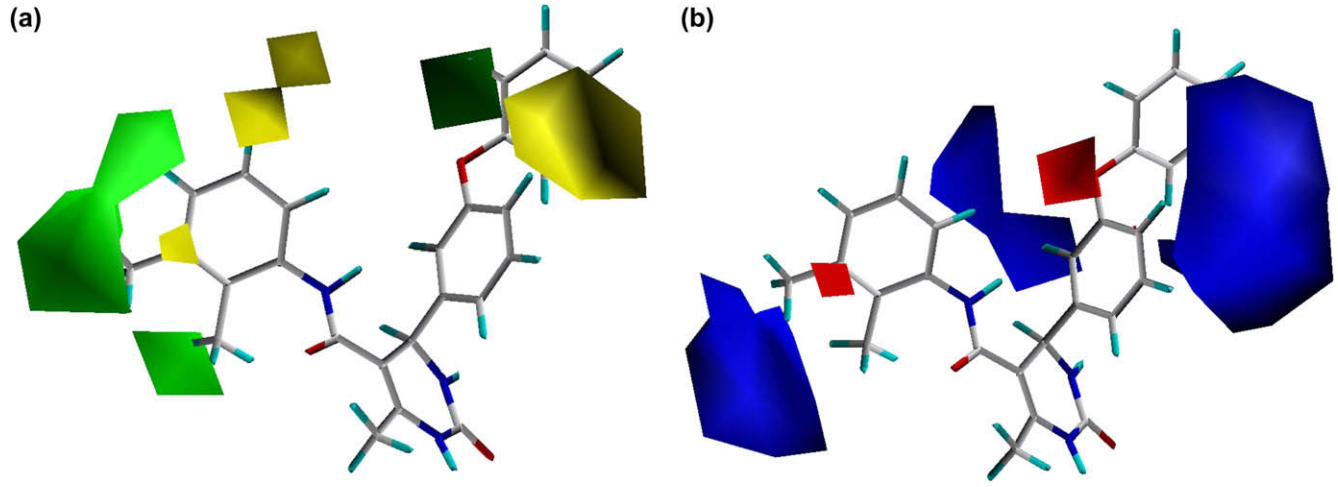

Fig. 3. The CoMFA contours around molecule **3c** (a) steric contours – favored (green); disfavored (yellow) (b) electrostatic contours – electropositive (blue); electronegative (red).

contours in Fig. 4e, in the vicinity of the 5-carboxamide, the *ortho* and *meta* position of the 5*N*-phenyl ring, while the favored magenta contours are found to encapsulate the *para* and *meta*′ positions of the 4-phenyl ring.

2.4. New molecules designed with improved activity

New molecules were designed on the basis of the contour maps seen around the most active molecule (**3c**). Variations (R_1, Table 4) were made on the 4-phenyl ring, at the *meta* position. Modifications (R_2, Table 4) were also made at the 5-carbamoyl group. It is seen that the molecules with R_2 groups of the type – 3-pyridyl and 4-pyridyl rings with suitable substituents, are predicted with higher activity than the correspondingly substituted phenyl rings. Further, molecules with pyridyl rings bearing nitro, dimethylaminocarbonyl, carbonyl or methoxy have greater activity than the molecules with unsubstituted pyridyl rings. Some of the newly designed molecules are depicted in Table 4.

3. Conclusions

The title compounds were obtained using the Biginelli reaction by reacting acetoacetanilide derivatives, substituted aldehydes and urea in methanol with a catalytic amount of conc. HCl. The synthesized compounds showed a range of antitubercular activity, extending from 2% to 63% inhibition of *M. tuberculosis*. The molecules were aligned in two ways, by the atom-fit and field-fit methods, and CoMFA and CoMSIA was carried out to map the structural features that modulate the inhibitory activity of these molecules. The CoMFA and CoMSIA models generated with the atom-fit alignment were better in terms of the statistical parameters (r^2, q^2 and r^2_{pred}) over the field-fit models. Analysis of the CoMFA and CoMSIA contours provide details on the fine relationship linking structure and activity, and offer clues for structural modifications that can improve the activity.

4. Experimental

4.1. Synthesis

Melting points were determined in open glass capillaries in a paraffin bath and are uncorrected. ^{1}H NMR spectra were recorded on a BRUKER AC 300 MHz FT-NMR spectrophotometer using tetramethylsilane as an internal standard. Mass spectra were recorded on JEOL SX 102/DA-6000 by the FAB (Fast Atom Bombardment) technique for ionization. Thin layer chromatography was performed on Merck Kieselgel 60F254 (Merck 5549, USA) plates.

4.2. General method for the preparation of *N*-phenyl-6-methyl-2-oxo-4-phenyl-1,2,3,4-tetrahydropyrimidine-5-carboxamide

Urea (0.9 g, 15 mmol), aldehyde (10 mmol) and acetoacetanilide (10 mmol) were taken in 10 mL of methanol in a 100 mL round bottom flask. The mixture was refluxed for 10 min when a clear solution resulted. Then 3–4 drops of conc. HCl were added to the solution. The reaction mixture was refluxed in a water bath for 5–10 h. The progress of the reaction was monitored by TLC. When the reaction was complete, the flask was removed from the water bath and allowed to cool to room temperature. The separated solid was collected by suction, washed with methanol and recrystallized from DMF.

4.2.1. *N*-(2,5-Dimethylphenyl)-6-methyl-2-oxo-4-(4-methoxyphenyl)-1,2,3,4-tetrahydropyrimidine-5-carboxamide (**3a**)

Mp 240–241 °C; yield 59%; ^{1}H NMR (DMSO-d_6, δ ppm): 1.59 (s, 3H), 1.78 (s, 3H), 2.67 (s, 3H), 3.04 (s, 3H), 5.33 (s, 1H), 6.79 (d, 2H; $J = 7.82$), 7.23 (m, 3H), 7.92 (dd, 2H; $J = 8.14$), 7.56 (s, 1H), 8.80 (s, 1H), 9.78 (s, 1H); IR (cm^{-1}): 3389 (N–H str.), 1667, 1710 (CO str.); Mass (*m*/*z*): 365 (M^+, 62%), 245 (100%); ^{13}C NMR (δ ppm): 11.39,

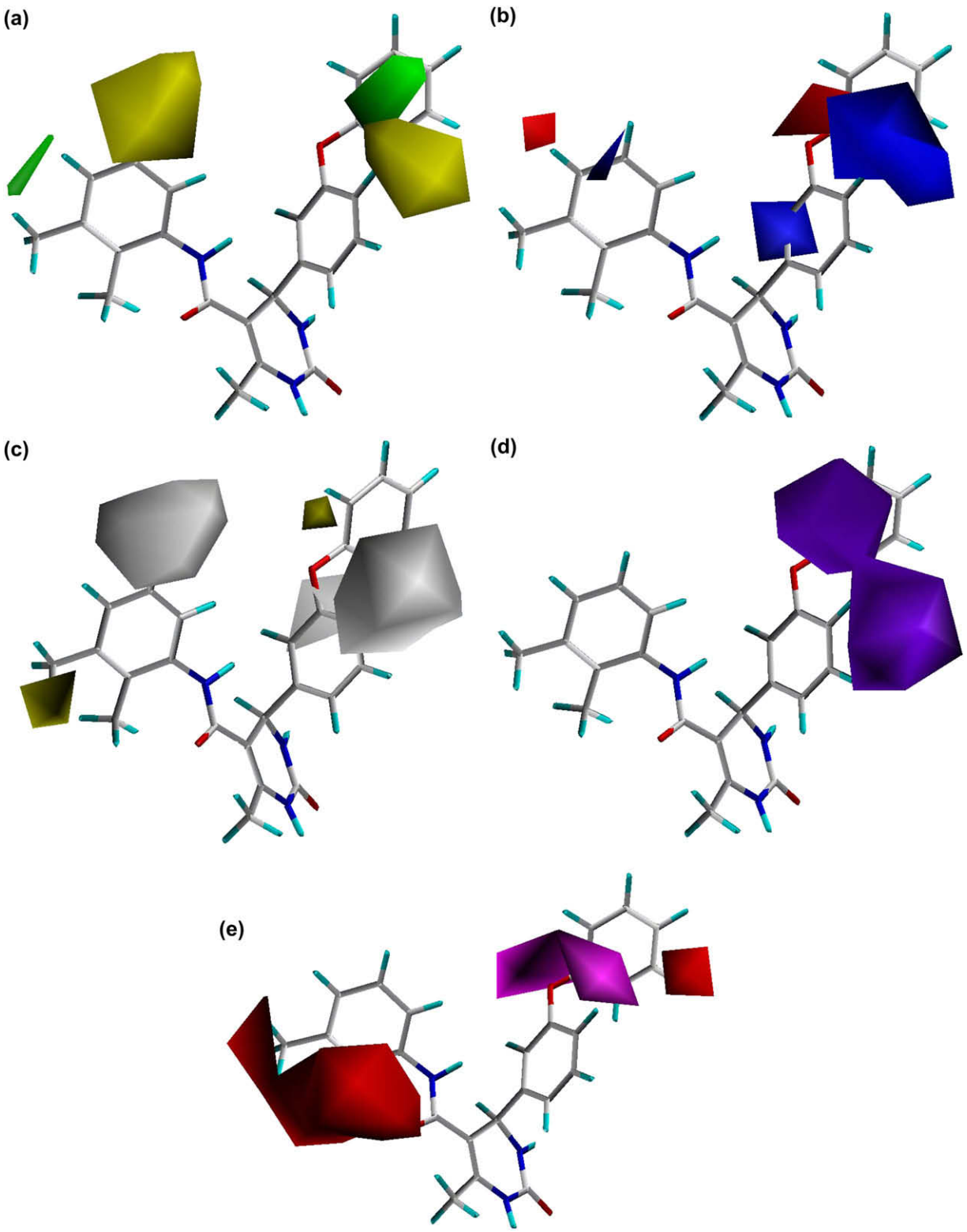

Fig. 4. The CoMSIA contours around molecule **3c** (a) steric contours – favored (green), disfavored (yellow) (b) electrostatic contours – electropositive (blue) electronegative (red) (c) hydrophobic contours – favored (yellow), disfavored (white) (d) H-donor contours – favored (cyan) (e) H-acceptor contours – favored (magenta), disfavored (purple), disfavored (red).

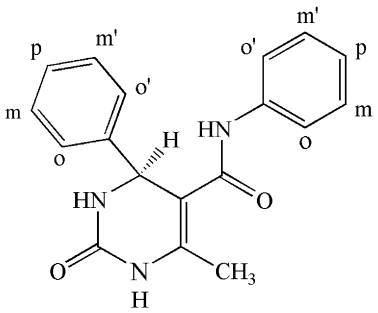

Fig. 5. The figure is used for explaining the CoMFA and CoMSIA.

17.23, 19.68, 49.12, 56.32, 109.31, 117.36, 117.88, 122.27, 123.39, 124.72, 126.39, 128.14, 134.32, 137.19, 138.43, 139.18, 148.13, 151.29, 152.32, 165.18. Anal. Calcd for $C_{21}H_{23}N_3O_3$: C 69.02, H 6.34, N 11.50; found: C 69.07, H 6.39, N 11.52.

*4.2.2. N-(2,5-Dimethylphenyl)-6-methyl-2-oxo-4-(3-phenoxyphenyl)-1,2,3,4-tetrahydro-pyrimidine-5-carboxamide (**3b**)*

Mp 258–261 °C; yield 60%; ^{1}H NMR (DMSO-d_6, δ ppm): 2.53 (s, 3H), 2.88 (s, 3H), 3.16 (s, 3H), 5.14 (s, 1H), 7.11 (d, 2H; $J = 7.69$), 7.53 (m, 4H), 7.82 (dd, 1H; $J = 7.82$), 7.96 (m, 2H), 8.14 (d, 1H; $J = 1.87$), 8.32 (dd, 2H; $J = 7.92, 2.14$), 8.03 (s, 1H), 8.61 (s, 1H), 9.79 (s, 1H); IR (cm^{-1}): 3411 (N–H str.), 1650, 1709 (CO str.); Mass (*m/z*): 427 (M^+, 82%), 307 (100%); ^{13}C NMR (δ ppm): 12.18, 16.11, 20.32, 53.18, 110.54, 116.32, 116.89, 118.18, 119.39, 123.88, 125.39, 125.92, 127.18, 128.92, 130.18, 130.72, 131.93, 134.35, 136.82, 137.13, 141.32, 148.19, 159.25, 163.18, 166.18, 168.32. Anal. Calcd for $C_{26}H_{25}N_3O_3$: C 73.05, H 5.89, N 9.83; found: C 73.08, H 5.92, N 9.85.

*4.2.3. N-(2,3-Dimethylphenyl)-6-methyl-2-oxo-4-(3-phenoxyphenyl)-1,2,3,4-tetrahydro-pyrimidine-5-carboxamide (**3c**)*

Mp 220–222 °C; yield 63%; ^{1}H NMR (DMSO-d_6, δ ppm): 2.12 (s, 3H), 2.42 (s, 3H), 2.53 (s, 3H), 5.56 (s, 1H), 7.54 (dd, 1H; $J = 8.22$), 7.89 (m, 7H), 8.12 (d, 1H; $J = 2.08$), 8.29 (d, 2H, $J = 7.78$), 8.40 (dd, 1H; $J = 7.61$), 7.72 (s, 1H), 8.86 (s, 1H), 9.23 (s, 1H); IR (cm^{-1}): 3439 (N–H str.), 1672, 1712 (CO str.); Mass (*m/z*): 427 (M^+, 68%), 307 (100%); ^{13}C NMR (δ ppm): 11.56, 15.28, 17.39, 50.23, 107.46, 112.34, 114.15, 116.29, 119.22, 122.78, 124.27, 125.39, 127.66, 129.32, 131.25, 132.34, 135.23, 136.11, 138.45, 140.10, 141.40, 147.18, 155.73, 159.27, 163.17, 170.42. Anal. Calcd for $C_{26}H_{25}N_3O_3$: C 73.05, H 5.89, N 9.83; found: C 73.11, H 5.92, N 9.91.

*4.2.4. N-(2-Chlorophenyl)-6-methyl-2-oxo-4-(2-nitrophenyl)-1,2,3,4-tetrahydro-pyrimidine-5-carboxamide (**3d**)*

Mp 196–198 °C; yield 60%; ^{1}H NMR ($CDCl_3$, δ ppm): 2.78 (s, 3H), 5.20 (s, 1H), 7.13 (t, 1H; $J = 8.26, 1.96$), 7.49 (t, 1H, $J = 7.84, 2.12$), 7.59 (s, 1H), 7.88 (m, 4H), 8.19 (dd, 1H; $J = 8.16, 1.79$), 8.26 (dd, 1H; $J = 8.10, 2.13$), 8.40 (s, 1H), 9.66 (s, 1H); IR (cm^{-1}): 3404 (N–H str.), 1669, 1711 (CO str.); Mass (*m/z*): 386 (M^+, 66%), 260 (100%); ^{13}C NMR (δ ppm): 13.17, 53.18, 106.34, 117.18, 122.34, 124.67, 125.97, 128.36, 129.34, 131.47, 134.25, 138.78, 142.15, 143.64, 148.57, 149.78, 153.62, 164.76. Anal. Calcd for $C_{18}H_{15}ClN_4O_4$: C 55.89, H 3.91, N 14.49; found: C 55.90, H 3.92, N 14.50.

*4.2.5. N-(2,5-Dimethylphenyl)-6-methyl-2-oxo-4-(4-nitrophenyl)-1,2,3,4-tetrahydro-pyrimidine-5-carboxamide (**3e**)*

Mp 140–142 °C; yield 56%; ^{1}H NMR (DMSO-d_6, δ ppm): 1.67 (s, 3H), 1.98 (s, 3H), 2.81 (s, 3H), 5.33 (s, 1H), 7.26 (dd, 2H; $J = 7.59, 2.21$), 7.68 (m, 5H), 7.99 (s, 1H), 8.37 (s, 1H), 9.92 (s, 1H); IR (cm^{-1}): 3440 (N–H str.), 1656, 1720 (CO str.); Mass (*m/z*): 380 (M^+, 62%), 260 (100%); ^{13}C NMR (δ ppm): 10.18, 14.47, 18.78, 58.27, 107.29, 112.86, 115.49, 120.37, 123.17, 124.88, 127.37, 129.19, 132.57, 135.71, 136.93, 141.48, 145.24, 148.68, 155.62, 171.68. Anal. Calcd for $C_{20}H_{20}N_4O_4$: C 63.15, H 5.30, N 14.73; found: C 63.19, H 5.32, N 14.76.

*4.2.6. N-(Phenyl)-6-methyl-2-oxo-4-(4-chlorophenyl)-1,2,3,4-tetrahydro-pyrimidine-5-carboxamide (**3f**)*

Mp 157–158 °C; yield 68%; ^{1}H NMR ($CDCl_3$, δ ppm): 2.45 (s, 3H), 5.22 (s, 1H), 6.78 (d, 2H; $J = 7.61$), 7.14 (m, 5H), 7.35 (d, 2H; $J = 8.37$), 7.44 (s, 1H), 8.55 (s, 1H), 9.36 (s, 1H); IR (cm^{-1}): 3472 (N–H str.), 1669, 1701 (CO str.); Mass (*m/z*): 341 (M^+, 77%), 249 (100%); ^{13}C NMR (δ ppm): 12.38, 61.29, 114.25, 123.27, 126.28, 127.33, 130.41, 132.26, 136.38, 137.78, 139.33, 144.23, 145.56, 148.26, 151.22, 155.28, 160.18, 167.28. Anal. Calcd for $C_{18}H_{16}ClN_3O_2$: C 63.25, H 4.72, N 12.29; found: C 63.29, H 4.75, N 12.30.

*4.2.7. N-(2-Flourophenyl)-6-methyl-2-oxo-4-(4-hydroxyphenyl)-1,2,3,4-tetrahydro-pyrimidine-5-carboxamide (**3g**)*

Mp 244–245 °C; yield 64%; ^{1}H NMR ($CDCl_3$-d_6, δ ppm): 3.79 (s, 3H), 5.19 (s, 1H), 6.84 (d, 2H; $J = 9.12$), 7.23 (m, 3H), 7.44 (t, 1H; $J = 8.81, 2.13$), 7.52 (d, 2H; $J = 9.53$), 7.60 (s, 1H), 8.95 (s, 1H), 9.39 (s, 1H), 10.41 (s, 1H); IR (cm^{-1}): 3393 (N–H str.), 1660, 1718 (CO str.); Mass (*m/z*): 341 (M^+, 67%), 231 (100%); ^{13}C NMR (δ ppm): 10.45, 57.24, 111.45, 116.76, 119.34, 127.34, 129.45, 133.56, 134.34, 137.24, 139.56, 140.22, 144.27, 145.39, 154.34, 159.36, 166.89, 173.26. Anal. Calcd for $C_{18}H_{16}FN_3O_3$: C 63.34, H 4.72, N 12.31; found: C 63.35, H 4.75, N 12.35.

*4.2.8. N-(2,5-Dichlorophenyl)-6-methyl-2-oxo-4-(4-nitrophenyl)-1,2,3,4-tetrahydro-pyrimidine-5-carboxamide (**3h**)*

Mp 246–247 °C; yield 56%; ^{1}H NMR ($CDCl_3$, δ ppm): 2.17 (s, 3H), 5.48 (s, 1H), 7.25 (m, 5H), 8.21 (d, 2H; $J = 7.76$), 7.82 (s, 1H), 9.00 (s, 1H), 9.27 (s, 1H); IR (cm^{-1}): 3214 (N–H str.), 1652, 1707 (CO str.); Mass (*m/z*): 421 (M^+, 59%), 260 (100%);

Table 4
New molecules with improved predicted activity

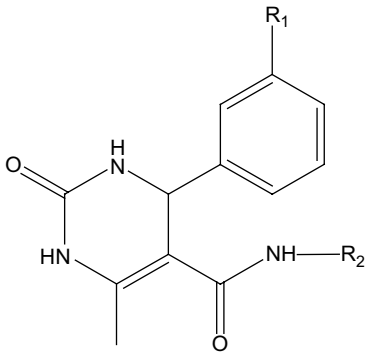

Sr. no.	Molecule	R_1	R_2	Predicted activity (CoMFA)[a]	Predicted activity (CoMSIA)[a]
1	N001	H	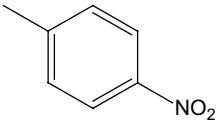	5.36	4.65
2	N002	$-OCONHCH_3$	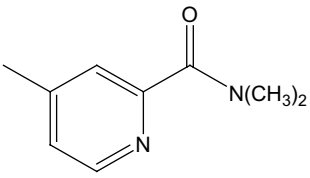	5.57	4.63
3	N003	$-COCH_3$	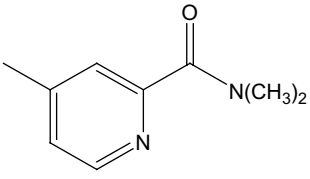	5.36	4.55
4	N004	$-CN$	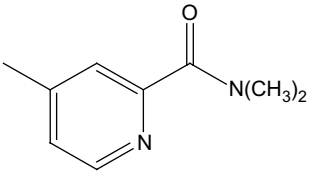	5.61	4.47
5	N005	$-NHSO_2CH_3$	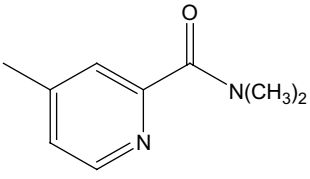	5.52	4.35
6	N006	$-CF_3$	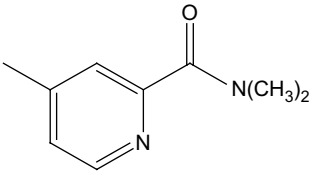	5.61	4.37

[a] Also see Tables 1 and 2 for comparison.

^{13}C NMR (δ ppm): 11.89, 48.35, 110.56, 118.39, 121.28, 126.34, 126.95, 130.24, 131.57, 134.25, 135.89, 137.43, 137.79, 145.28, 148.27, 150.28, 156.35, 167.37. Anal. Calcd for $C_{18}H_{14}Cl_2N_4O_4$: C 51.32, H 3.35, N 13.30; found: C 51.39, H 3.39, N 13.38.

*4.2.9. N-(2,4-Dimethylphenyl)-6-methyl-2-oxo-4-(4-hydroxyphenyl)-1,2,3,4-tetrahydro-pyrimidine-5-carboxamide (**3i**)*

Mp 215–216 °C; yield 56%; ^{1}H NMR (DMSO-d_6, δ ppm): 1.47 (s, 3H), 1.73 (s, 3H), 3.14 (s, 3H), 5.23 (s, 1H), 6.69–7.92

(m, 7H), 7.54 (s, 1H), 8.12 (s, 1H), 9.58 (s, 1H), 10.34 (s, 1H); IR (cm^{-1}): 3425 (N–H str.), 1655, 1717 (CO str.); Mass (*m/z*): 351 (M^+, 54%), 231 (100%); ^{13}C NMR (δ ppm): 13.34, 17.25, 19.28, 64.23, 118.23, 118.78, 122.34, 126.36, 127.58, 133.23, 134.74, 136.47, 138.49, 140.25, 141.28, 144.24, 148.35, 158.13, 159.37, 165.36. Anal. Calcd for $C_{20}H_{21}N_3O_3$: C 68.36, H 6.02, N 11.96; found: C 68.38, H 6.03, N 11.98.

*4.2.10. N-(3-Nitrophenyl)-6-methyl-2-oxo-4-(4-hydroxyphenyl)-1,2,3,4-tetrahydro-pyrimidine-5-carboxamide (**3j**)*

Mp 206–208 °C; yield 52%; ^1H NMR ($CDCl_3$, δ ppm): 2.55 (s, 3H), 5.34 (s, 1H), 7.19 (t, 1H; $J = 8.67$), 7.48 (m, 5H), 7.69 (dd, 2H, $J = 7.19$, 2.19), 7.85 (s, 1H), 8.33 (s, 1H), 9.47 (s, 1H), 10.78 (s, 1H); IR (cm^{-1}): 3239 (N–H str.), 1662, 1711 (CO str.); Mass (*m/z*): 368 (M^+, 52%), 231 (100%); ^{13}C NMR (δ ppm): 10.37, 46.18, 108.27, 118.25, 119.59, 126.27, 128.36, 131.26, 135.38, 136.72, 139.37, 139.88, 142.36, 146.78, 152.46, 158.48, 163.59, 172.48. Anal. Calcd for $C_{18}H_{16}N_4O_5$: C 58.69, H 4.38, N 15.21; found: C 58.74, H 4.43, N 15.27.

*4.2.11. N-(3-Chloro-4-flourophenyl)-6-methyl-2-oxo-4-(3-chlorophenyl)-1,2,3,4-tetrahydro-pyrimidine-5-carboxamide (**3k**)*

Mp 270–272 °C; yield 65%; ^1H NMR ($CDCl_3$, δ ppm): 3.12 (s, 3H), 5.12 (s, 1H), 6.85 (d, 1H; $J = 9.92$), 7.34 (m, 4H), 7.45 (dd, 1H; $J = 7.25$, 3.87), 7.78 (d, 1H; $J = 9.43$), 7.93 (s, 1H), 8.21 (s, 1H), 9.03 (s, 1H); IR (cm^{-1}): 3256 (N–H str.), 1658, 1708 (CO str.); Mass (*m/z*): 394 (M^+, 68%), 249 (100%); ^{13}C NMR (δ ppm): 14.26, 67.37, 110.38, 117.35, 118.27, 121.29, 125.26, 125.81, 129.69, 130.33, 133.16, 135.93, 138.24, 140.36, 144.28, 147,84, 154.29, 166.73. Anal. Calcd for $C_{18}H_{15}Cl_2FN_3O_2$: C 54.84, H 3.58, N 10.66; found: C 54.88, H 3.59, N 10.70.

*4.2.12. N-(2-Flourophenyl)-6-methyl-2-oxo-4-(4-nitrophenyl)-1,2,3,4-tetrahydro-pyrimidine-5-carboxamide (**3l**)*

Mp 254–255 °C; yield 60%; ^1H NMR ($CDCl_3$, δ ppm): 2.79 (s, 3H), 5.07 (s, 1H), 6.70 (dd, 2H; $J = 8.94$, 2.31), 7.29 (s, 1H), 7.54 (m, 5H), 7.90 (t, 1H; $J = 9.85$), 8.66 (s, 1H), 9.89 (s, 1H); IR (cm^{-1}): 3405 (N–H str.), 1678, 1702 (CO str.); Mass (*m/z*): 370 (M^+, 67%), 260 (100%); ^{13}C NMR (δ ppm): 12.44, 49.24, 112.23, 115.44, 118.37, 122.18, 126.28, 131.28, 134.54, 138.55, 139.83, 140.89, 142.57, 148.29, 149.70, 153.46, 158.36, 170.78. Anal. Calcd for $C_{18}H_{15}FN_4O_4$: C 58.38, H 4.08, N 15.13; found: C 58.42, H 4.09, N 15.15.

*4.2.13. N-(3,4-Dimethylphenyl)-6-methyl-2-oxo-4-(4-nitrophenyl)-1,2,3,4-tetrahydro-pyrimidine-5-carboxamide (**3m**)*

Mp 254–256 °C; yield 58%; ^1H NMR (DMSO-d_6, δ ppm): 1.23 (s, 3H), 1.67 (s, 3H), 2.78 (s, 3H), 5.48 (s, 1H), 6.89 (dd, 1H; $J = 8.11$, 2.32), 7.11 (m, 3H), 7.38 (d, 2H; $J = 8.94$), 7.54 (s, 1H), 8.14 (d, 1H; $J = 7.17$), 8.52 (s, 1H), 9.84 (s, 1H); IR (cm^{-1}): 3289 (N–H str.), 1678, 1706 (CO str.); Mass (*m/z*): 380 (M^+, 54%), 260 (100%); ^{13}C NMR (δ ppm): 11.68, 14.38, 19.45, 62.67, 108.57, 117.68, 118.95, 121.33, 124.52, 128.88, 130.07, 130.68, 134.78, 138.42, 141.38, 142.39, 145.49, 147.22, 154.79, 167.58. Anal. Calcd for $C_{20}H_{20}N_4O_4$: C 63.15, H 5.30, N 14.73; found: C 63.19, H 5.31, N 14.75.

*4.2.14. N-(2,4-Dimethylphenyl)-6-methyl-2-oxo-4-(4-nitrophenyl)-1,2,3,4-tetrahydro-pyrimidine-5-carboxamide (**3n**)*

Mp 215–216 °C; yield 56%; ^1H NMR (DMSO-d_6, δ ppm): 1.08 (s, 3H), 1.93 (s, 3H), 2.79 (s, 3H), 5.69 (s, 1H), 6.92 (d, 1H; $J = 7.64$), 7.29 (m, 4H), 7.78 (d, 2H; $J = 8.35$), 7.94 (s, 1H), 8.72 (s, 1H), 9.48 (s, 1H); IR (cm^{-1}): 3321 (N–H str.), 1689, 1709 (CO str.); Mass (*m/z*): 380 (M^+, 62%), 260 (100%); ^{13}C NMR (δ ppm): 14.63, 17.28, 18.39, 65.61, 112.78, 117.28, 121.37, 122.84, 123.35, 124.19, 130.68, 134.24, 137.82, 138.27, 140.21, 142.56, 143.93, 147.41, 152.84, 161.84. Anal. Calcd for $C_{20}H_{20}N_4O_4$: C 63.15, H 5.30, N 14.73; found: C 63.17, H 5.33, N 14.75.

*4.2.15. N-(2-Chlorophenyl)-6-methyl-2-oxo-4-(3-nitrophenyl)-1,2,3,4-tetrahydro-pyrimidine-5-carboxamide (**3o**)*

Mp 245–246 °C; yield 62%; ^1H NMR ($CDCl_3$, δ ppm): 2.79 (s, 3H), 5.59 (s, 1H), 7.02 (t, 1H; $J = 8.18$), 7.45 (m, 7H), 8.53 (s, 1H), 8.79 (s, 1H), 9.70 (s, 1H); IR (cm^{-1}): 3447 (N–H str.), 1659, 1701 (CO str.); Mass (*m/z*): 386 (M^+, 72%), 260 (100%); ^{13}C NMR (δ ppm): 13.72, 45.74, 104.27, 112.35, 113.86, 118.25, 119.20, 124.37, 127.81, 130.34, 133.16, 136.68, 137.28, 139.50, 142.47, 151.74, 158.58, 167.38. Anal. Calcd for $C_{18}H_{15}ClN_4O_4$: C 55.89, H 3.91, N 14.49; found: C 55.95, H 3.98, N 14.55.

*4.2.16. N-(3-Chloro-4-flourophenyl)-6-methyl-2-oxo-4-(3-nitrophenyl)-1,2,3,4-tetrahydro-pyrimidine-5-carboxamide (**3p**)*

Mp 208–209 °C; yield 67%; ^1H NMR ($CDCl_3$, δ ppm): 2.89 (s, 3H), 5.47 (s, 1H), 7.12 (t, 1H; $J = 9.18$), 7.38 (m, 5H), 7.89 (d, 1H; $J = 9.37$), 7.98 (s, 1H), 8.78 (s, 1H), 9.82 (s, 1H); IR (cm^{-1}): 3439 (N–H str.), 1672, 1720 (CO str.); Mass (*m/z*): 404 (M^+, 70%), 260 (100%); ^{13}C NMR (δ ppm): 15.27, 57.16, 110.47, 118.24, 119.37, 122.49, 123.62, 128.89, 129.17, 134.58, 136.83, 139.42, 140.07, 146.47, 149.85, 157.31, 159.40, 171.37. Anal. Calcd for $C_{18}H_{14}ClFN_4O_3$: C 53.41, H 3.49, N 13.84; found: C 53.48, H 3.54, N 13.86.

*4.2.17. N-(2-Flourophenyl)-6-methyl-2-oxo-4-(3-nitrophenyl)-1,2,3,4-tetrahydro-pyrimidine-5-carboxamide (**3q**)*

Mp 210–212 °C; yield 62%; ^1H NMR ($CDCl_3$, δ ppm): 2.81 (s, 3H), 5.27 (s, 1H), 7.12 (s, 1H), 7.22 (t, 1H; $J = 9.18$), 7.39 (t, 1H; $J = 8.62$), 7.80 (m, 4H), 8.11 (dd, 1H; $J = 7.14$, 2.10), 8.28 (dd, 1H; $J = 9.23$, 3.92), 8.40 (s, 1H), 9.90 (s, 1H); IR (cm^{-1}): 3419 (N–H str.), 1667, 1712 (CO str.); Mass (*m/z*): 370 (M^+, 72%), 260 (100%); ^{13}C NMR (δ ppm): 13.48, 53.41, 113.68, 115.27, 121.57, 122.31, 127.63, 128.93, 132.30, 132.78,

136.74, 137.96, 143.52, 148.58, 150.41, 156.84, 163.45, 173.37. Anal. Calcd for $C_{18}H_{15}FN_4O_3$: C 58.38, H 4.08, N 15.13; found: C 58.45, H 4.11, N 15.16.

*4.2.18. N-(4-Flourophenyl)-6-methyl-2-oxo-4-(3-chlorophenyl)-1,2,3,4-tetrahydro-pyrimidine-5-carboxamide (**3r**)*

Mp 270–272 °C; yield 65%; ^{1}H NMR ($CDCl_3$, δ ppm): 2.86 (s, 3H), 5.35 (s, 1H), 6.88 (d, 2H; $J = 9.36$), 7.03 (t, 1H; $J = 7.84$, 1.78), 7.11 (d, 1H; $J = 9.17$), 7.45 (m, 3H), 7.62 (d, 2H; $J = 9.75$), 7.97 (s, 1H), 8.81 (s, 1H), 9.43 (s, 1H); IR (cm^{-1}): 3266 (N–H str.), 1652, 1713 (CO str.); Mass (*m/z*): 359 (M^+, 68%), 249 (100%); ^{13}C NMR (δ ppm): 12.84, 62.38, 105.25, 116.26, 117.83, 120.38, 121.26, 127.58, 129.38, 130.87, 133.28, 133.86, 137.39, 139.16, 141.29, 142.64, 157.49, 168.31; Anal. Calcd for $C_{18}H_{15}ClFN_3O_2$: C 60.09, H 4.20, N 11.68; found: C 60.14, H 4.25, N 11.70.

*4.2.19. N-(4-Methoxy-phenyl)-6-methyl-2-oxo-4-(4-nitrophenyl)-1,2,3,4-tetrahydro-pyrimidine-5-carboxamide (**3s**)*

Mp 268–270 °C; yield 62%; ^{1}H NMR ($CDCl_3$, δ ppm): 1.96 (s, 3H), 2.69 (s, 3H), 5.46 (s, 1H), 6.82 (d, 2H; $J = 9.12$), 7.52 (m, 4H), 7.79 (d, 2H; $J = 7.93$), 7.97 (s, 1H), 8.57 (s, 1H), 9.52 (s, 1H); IR (cm^{-1}): 3418 (N–H str.), 1675, 1713 (CO str.); Mass (*m/z*): 382 (M^+, 74%), 260 (100%); ^{13}C NMR (δ ppm): 15.74, 42.78, 56.82, 104.28, 110.28, 113.64, 116.92, 117.31, 119.48, 124.51, 127.75, 128.82, 129.30, 132.41, 136.78, 137.92, 144.58, 154.83, 168.91. Anal. Calcd for $C_{19}H_{18}N_4O_5$: C 59.68, H 4.74, N 14.65; found: C 59.73, H 4.75, N 14.68.

*4.2.20. N-(4-Chlorophenyl)-6-methyl-2-oxo-4-(3-nitrophenyl)-1,2,3,4-tetrahydro-pyrimidine-5-carboxamide (**3t**)*

Mp 210–212 °C; yield 62%; ^{1}H NMR ($CDCl_3$, δ ppm): 2.51 (s, 3H), 5.21 (s, 1H), 6.78 (d, 2H; $J = 8.89$), 7.13 (m, 5H), 7.36 (t, 1H; $J = 9.17$, 2.18), 7.61 (s, 1H), 8.37 (s, 1H), 9.60 (s, 1H); IR (cm^{-1}): 3413 (N–H str.), 1654, 1702 (CO str.); Mass (*m/z*): 386 (M^+, 72%), 260 (100%); ^{13}C NMR (δ ppm): 16.28, 49.53, 110.25, 114.38, 114.88, 123.47, 124.63, 127.36, 128.29, 130.05, 130.62, 135.58, 136.91, 138.43, 140.04, 152.36, 160.13, 167.33. Anal. Calcd for $C_{18}H_{15}ClN_4O_4$: C 55.89, H 3.91, N 14.49; found: C 55.94, H 3.94, N 14.56.

*4.2.21. N-(4-Methylphenyl)-6-methyl-2-oxo-4-(3-nitrophenyl)-1,2,3,4-tetrahydro-pyrimidine-5-carboxamide (**3u**)*

Mp 210–212 °C; yield 62%; ^{1}H NMR (DMSO-d_6, δ ppm): 2.91 (s, 3H), 5.48 (s, 1H), 6.79 (d, 2H; $J = 8.52$), 7.28 (m, 5H), 7.70 (t, 1H; $J = 9.13$, 1.88), 7.92 (s, 1H), 8.28 (s, 1H), 9.19 (s, 1H); IR (cm^{-1}): 3323 (N–H str.), 1680, 1700 (CO str.); Mass (*m/z*): 366 (M^+, 72%), 260 (100%); ^{13}C NMR (δ ppm): 12.73, 18.38, 58.91, 108.64, 117.83, 118.07, 122.38, 124.08, 127.48, 128.35, 131.26, 132.82, 135.37, 137.39, 139.70, 140.16, 142.47, 156.30, 171.04. Anal. Calcd for $C_{19}H_{18}N_4O_4$: C 62.29, H 4.95, N 15.29; found: C 62.34, H 4.96, N 15.31.

*4.2.22. N-(4-Flourophenyl)-6-methyl-2-oxo-4-(3-nitrophenyl)-1,2,3,4-tetrahydro-pyrimidine-5-carboxamide (**3v**)*

Mp 256–258 °C; yield 60%; ^{1}H NMR ($CDCl_3$, δ ppm): 2.86 (s, 3H), 5.62 (s, 1H), 6.92 (d, 2H; $J = 9.82$), 7.34 (m, 6H), 7.81 (s, 1H), 8.65 (s, 1H), 9.14 (s, 1H); IR (cm^{-1}): 3382 (N–H str.), 1669, 1716 (CO str.); Mass (*m/z*): 370 (M^+, 76%), 260 (100%); ^{13}C NMR (δ ppm): 14.27, 51.62, 111.64, 118.20, 118.94, 120.69, 121.38, 124.51, 125.82, 129.48, 130.26, 132.19, 136.29, 137.74, 138.15, 146.58, 154.27, 168.18. Anal. Calcd for $C_{18}H_{15}FN_4O_4$: C 58.38, H 4.08, N 15.13; found: C 58.40, H 4.10, N 15.17.

*4.2.23. N-(2-Methylphenyl)-6-methyl-2-oxo-4-(3-nitrophenyl)-1,2,3,4-tetrahydro-pyrimidine-5-carboxamide (**4a**)*

Mp 176–177 °C; yield 60%; ^{1}H NMR (DMSO-d_6, δ ppm): 1.82 (s, 3H), 2.28 (s, 3H), 5.40 (s, 1H), 7.06 (t, 1H; $J = 9.72$, 1.86), 7.23 (m, 5H), 7.49 (t, 1H; $J = 7.29$, 2.13), 7.71 (t, 1H; $J = 8.12$, 1.76), 7.81 (s, 1H), 8.78 (s, 1H), 9.08 (s, 1H); IR (cm^{-1}): 3449 (N–H str.), 1662, 1707 (CO str.); Mass (*m/z*): 366 (M^+, 80%), 260 (100%); ^{13}C NMR (δ ppm): 15.27, 17.80, 59.68, 107.28, 116.69, 117.25, 119.95, 120.31, 122.86, 124.58, 125.97, 129.47, 130.62, 132.61, 135.82, 138.14, 141.37, 152.81, 166.73. Anal. Calcd for $C_{19}H_{18}N_4O_4$: C 62.29, H 4.95, N 15.29; found: C 62.32, H 4.97, N 14.33.

*4.2.24. N-(2-Chlorophenyl)-6-methyl-2-oxo-4-(4-chlorophenyl)-1,2,3,4-tetrahydro-pyrimidine-5-carboxamide (**4b**)*

Mp 208–210 °C; yield 66%; ^{1}H NMR ($CDCl_3$, δ ppm): 2.13 (s, 3H), 5.89 (s, 1H), 7.11 (d, 2H; $J = 9.18$), 7.43 (t, 1H; $J = 7.13$), 7.67 (m, 5H), 7.82 (s, 1H), 8.64 (s, 1H), 9.92 (s, 1H); IR (cm^{-1}): 3376 (N–H str.), 1660, 1718 (CO str.); Mass (*m/z*): 376 (M^+, 81%), 249 (100%); ^{13}C NMR (δ ppm): 12.38, 65.82, 112.45, 115.28, 117.95, 120.32, 121.37, 124.53, 125.78, 128.13, 129.60, 130.27, 134.27, 137.82, 138.69, 140.24, 157.22, 169.41. Anal. Calcd for $C_{18}H_{15}Cl_2N_3O_2$: C 57.46, H 4.02, N 11.17; found: C 57.49, H 4.05, N 11.20.

*4.2.25. N-(4-Chlorophenyl)-6-methyl-2-oxo-4-(4-nitrophenyl)-1,2,3,4-tetrahydro-pyrimidine-5-carboxamide (**4c**)*

Mp 294–295 °C; yield 64%; ^{1}H NMR ($CDCl_3$, δ ppm): 2.92 (s, 3H), 5.56 (s, 1H), 6.78 (m, 2H), 7.26 (m, 4H), 7.92 (d, 2H; $J = 7.80$), 7.45 (s, 1H), 8.78 (s, 1H), 9.44 (s, 1H); IR (cm^{-1}): 3444 (N–H str.), 1652, 1719 (CO str.); Mass (*m/z*): 386 (M^+, 61%), 260 (100%); ^{13}C NMR (δ ppm): 14.92, 48.51, 104.38, 111.92, 114.68, 118.79, 119.27, 120.27, 125.31, 126.84, 128.38, 129.48, 131.18, 135.39, 136.35, 145.28, 153.14, 163.89. Anal. Calcd for $C_{18}H_{15}ClN_4O_4$: C 55.89, H 3.91, N 14.49; found: C 55.92, H 3.94, N 14.51.

*4.2.26. N-(3,4-Dimethylphenyl)-6-methyl-2-oxo-4-(3-phenoxyphenyl)-1,2,3,4-tetrahydro-pyrimidine-5-carboxamide (**4d**)*

Mp 224–225 °C; yield 59%; ^{1}H NMR (DMSO-d_6, δ ppm): 2.24 (s, 3H), 2.67 (s, 3H), 3.12 (s, 3H), 5.76 (s, 1H), 7.12 (dd, 1H; $J = 7.35$, 2.12), 7.39 (d, 1H; $J = 9.72$), 7.43 (m, 6H), 7.58 (m, 3H), 7.68 (s, 1H), 7.79 (t, 1H; $J = 8.15$), 8.46 (s, 1H), 9.12 (s, 1H); IR (cm^{-1}): 3378 (N–H str.), 1664, 1710 (CO str.); Mass (*m/z*): 427 (M^+, 62%), 307 (100%); ^{13}C NMR (δ ppm): 13.58, 17.25, 19.46, 56.82, 108.25, 112.38, 113.39, 116.78, 118.29, 121.57, 122.36, 126.28, 127.92, 128.47, 132.31, 134.83, 135.79, 138.26, 139.41, 140.66, 142.28, 143.86, 152.42, 155.82, 160.12, 169.31. Anal. Calcd for $C_{26}H_{25}N_3O_3$: C 73.05, H 5.89, N 9.83; found: C 73.08, H 5.90, N 9.89.

*4.2.27. N-(Phenyl)-6-methyl-2-oxo-4-(4-nitrophenyl)-1,2,3,4-tetrahydro-pyrimidine-5-carboxamide (**4e**)*

Mp 304–306 °C; yield 64%; ^{1}H NMR ($CDCl_3$, δ ppm): 1.83 (s, 3H), 5.23 (s, 1H), 6.69 (dd, 2H; $J = 8.49$, 1.82), 7.04 (m, 2H), 7.38 (m, 3H), 7.59 (t, 2H; $J = 7.47$, 2.31), 7.88 (s, 1H), 8.29 (s, 1H), 9.57 (s, 1H); IR (cm^{-1}): 3337 (N–H str.), 1684, 1712 (CO str.); Mass (*m/z*): 352 (M^+, 67%), 260 (100%); ^{13}C NMR (δ ppm): 11.73, 58.12, 103.67, 114.57, 115.69, 121.73, 122.98, 126.26, 128.94, 129.24, 132.16, 133.83, 135.78, 138.38, 139.21, 145.73, 151.69, 164.47. Anal. Calcd for $C_{18}H_{16}N_4O_4$: C 61.36, H 4.58, N 15.90; found: C 61.40, H 4.60, N 15.94.

*4.2.28. N-(3,4-Dimethylphenyl)-6-methyl-2-oxo-4-(3-nitrophenyl)-1,2,3,4-tetrahydro-pyrimidine-5-carboxamide (**4f**)*

Mp 220–222 °C; yield 63%; ^{1}H NMR (DMSO-d_6, δ ppm): 2.07 (s, 3H), 2.59 (s, 3H), 2.90 (s, 3H), 5.59 (s, 1H), 6.89 (m, 3H), 7.56 (m, 4H), 7.74 (s, 1H), 8.66 (s, 1H), 9.41 (s, 1H); IR (cm^{-1}): 3429 (N–H str.), 1662, 1707 (CO str.); Mass (*m/z*): 380 (M^+, 68%), 260 (100%); ^{13}C NMR (δ ppm): 12.35, 14.78, 18.24, 50.12, 111.37, 117.45, 118.28, 120.28, 123.52, 124.85, 125.89, 131.25, 134.58, 135.80, 136.27, 138.62, 139.36, 147.48, 153.45, 168.21. Anal. Calcd for $C_{20}H_{20}N_4O_4$: C 63.15, H 5.30, N 14.73; found: C 63.17, H 5.31, N 14.76.

*4.2.29. N-(3-Chloro-4-flouro-phenyl)-6-methyl-2-oxo-4-(4-nitrophenyl)-1,2,3,4-tetrahydro-pyrimidine-5-carboxamide (**4g**)*

Mp 262–264 °C; yield 59%; ^{1}H NMR ($CDCl_3$, δ ppm): 1.96 (s, 3H), 5.67 (s, 1H), 6.90 (d, 1H; $J = 9.12$), 7.27 (m, 2H), 7.48 (m, 2H), 7.67 (s, 1H), 7.87 (d, 2H; $J = 7.14$), 8.77 (s, 1H), 9.94 (s, 1H); IR (cm^{-1}): 3312 (N–H str.), 1657, 1705 (CO str.); Mass (*m/z*): 404 (M^+, 63%), 260 (100%); ^{13}C NMR (δ ppm): 14.56, 53.58, 112.37, 117.28, 119.48, 120.31, 122.89, 125.37, 126.19, 128.25, 129.39, 130.17, 134.68, 135.69, 137.27, 148.16, 152.84, 164.64. Anal. Calcd for $C_{18}H_{14}ClFN_4O_4$: C 53.41, H 3.49, N 13.84; found: C 53.45, H 3.53, N 13.90.

4.3. Antitubercular activity

Antitubercular activity was determined using the BACTEC 460 system [42] modified as described below. Stock solutions as test compounds were prepared in dimethylsulfoxide (DMSO) at 1 mg/mL and sterilized by passage through 0.22 μm PFTE filters (Millex-FG, Millipore, Bedford MA). Fifty microliters was added to 4 mL radiometric 7H12 broth (BACTEC 12B; Bectron Dickinson Diagnostic Instrument system, Sparks, MD) to achieve a final concentration of 6.25 mg/mL. Controls received 50 mL DMSO. Rifampin (Sigma Chemical Co., St. Louis, MO) was included as a positive drug control. Rifampin was solubilized and diluted in DMSO and added to BACTEC-12 broth to achieve minimum inhibitory concentration (MIC, lowest concentration inhibiting 99% of the inoculums).

M. tuberculosis H37Rv strain (ATCC 27294; American type culture collection, Rockville, MD) was cultured at 37 °C on a rotary shaker in middle brook 7H9 broth (Difco Laboratories, Detroit, MI) supplemented with 0.2 v/v glycerol and 0.05% v/v Tween 80 until the culture turbidity achieved an optical density of 0.45–0.55 at 550 nm. Bacteria were pelleted by centrifugation, washed twice and resuspended in one-fifth of the original volume in Dulbecoo's phosphate buffered saline [PBS, Irvine Scientific, Santa Ana, (A)]. Large bacterial clumps were removed by passage through an 8 mm filter (Malgene, Rochester, NY) and aliquots were frozen at −80 °C. The cultures were thawed and an appropriate dilution performed such that a BACTEC-12B vial inoculated with a 0.1 mL would reach a growth index (GI) of 999 in 5 days. One-tenth of the diluted inoculum was used to inoculate 4 mL fresh BACTEC-12B broth containing the test compounds. An additional control vial was included which received a further 1:100 diluted inoculum (as well as 50 mL DMSO) for use in calculating the MIC of rifampicin, respectively, by established procedures.

Cultures were incubated at 37 °C and the Growth of Inhibition (GI) determined daily until control cultures acheived a GI of 999. Assays were usually completed in 5–8 days. Percentage inhibition was defined as 1–(GI of test sample/GI of control) 10. Minimum inhibitory concentration of compound effecting a reduction in daily change in GI, which was less than that observed with a 1:100 diluted control culture on day the later reached a GI of at least 30.

Acknowledgement

Authors are thankful to the Tuberculosis Antimicrobial Acquisition and Coordinating Facility (TAACF), USA for antitubercular screening and to the Department of Chemistry, Saurashtra University, Rajkot for providing laboratory facilities. The computational facilities at Bombay College of Pharmacy, Mumbai were supported by All India Council of Technical Education (F. No. 8022/RID/NPROJ/RPS-5/2003-04).

References

[1] C. Dye, S. Scheele, R. Dolin, V. Pathania, M. Raviglione, J. Am. Med. Assoc. (1999) 677–686.
[2] T.H. Frieden, T.H. Sterling, S.S. Munsiff, C.J. Watt, C. Dye, Lancet 362 (2003) 887–899.
[3] Tuberculosis Facts, WHO, 2006.
[4] M.A. Espinal, Tuberculosis 83 (2003) 44–51.
[5] K. Johnsson, P.G. Schultz, J. Am. Chem. Soc. 116 (1994) 7425–7426.
[6] A. Rattan, A. Kalia, N. Ahmad, Emerg. Infect. Dis. 4 (1998) 195–209.
[7] T. Bodmer, K. Zurcher, P. Imboden, A. Telenti, J. Antimicrob. Chemother. 35 (1995) 345–348.
[8] A.C. Fluit, M.R. Visser, R.J. Schmitz, Clin. Microbiol. Rev. 14 (2001) 836–871.
[9] A. Nayyar, R. Jain, Curr. Med. Chem. 12 (2005) 1873–1886.
[10] C.K. Stover, P. Warrener, D.R. Vandevanter, D.R. Sherman, T.N. Arain, M.H. Langhorne, S.W. Anderson, J.A. Towell, Y. Yuan, D.N. McMurry, B.N. Kreiswirth, C.E. Barry, B.R. Baker, Nature 405 (2000) 962–966.
[11] W.R. Baker, C. Shaopei, E.L. Keeler, US Patent 6,087,358-A, 2000.
[12] R. Pathak, C.S. Pant, A.K. Shaw, A.P. Bhanduri, A.N. Gaikwad, S. Sinha, A. Srivastava, K.K. Srivastava, V. Chaturvedi, R. Srivastava, B.S. Srivastava, Bioorg. Med. Chem. 10 (2002) 3187–3196.
[13] D.G. Rando, D.N. Sato, L. Siqueira, A. Malvezzi, C.Q.F. Leite, A.T. Amaral, E.I. Ferreira, L.C. Tavaresa, Bioorg. Med. Chem. 10 (2002) 557–560.
[14] T.C. McKee, C.D. Covington, R.W. Fuller, H.R. Bokesch, S. Young, J.H. Cardellina, M.R. Kadushin, D.D. Soejarto, P.F. Stevens, C.M. Cragg, M.R. Boyd, J. Nat. Prod. 61 (1998) 1252–1256.
[15] C. Spino, M. Dodier, S. Sotheeswaran, Bioorg. Med. Chem. Lett. 8 (1998) 3475–3478.
[16] A.K. Bakkestuen, L.L. Gundersen, G. Langli, F. Liu, J.M. Nolsoe, Bioorg. Med. Chem. Lett. 10 (2000) 1207–1219.
[17] L.L. Gundersen, J. Nissen-Meyer, B. Spilsberg, J. Med. Chem. 45 (2002) 1383–1386.
[18] M. Biava, R. Fioravanti, G.C. Porretta, D. Deidda, C. Maullu, R. Pompei, Bioorg. Med. Chem. Lett. 9 (1999) 2983–2988.
[19] R. Ragno, G.R. Marshall, R.D. Santo, R. Costi, S. Massa, R. Pompei, M. Artico, Bioorg. Med. Chem. 8 (2000) 1423–1432.
[20] K. Waisser, J. Gregor, L. Kubicova, V. Klimesova, J. Kunes, M. Machacek, J. Kaustova, Eur. J. Med. Chem. 35 (2000) 733–741.
[21] A. Ulubelen, G. Topcu, C.B. Johansson, J. Nat. Prod. 60 (1997) 1275–1280.
[22] G.A. Wachter, J. Nat. Prod. 61 (1998) 965–968.
[23] D. Ubiali, G. Pagani, M. Pregnolato, C. Piersimoni, J.P. Munoz, A.R. Gascon, M. Terreni, Bioorg. Med. Chem. Lett. 12 (2002) 2541–2544.
[24] K. Waisser, K. Drazkova, J. Kunes, V. Klimesova, J. Kaustova, Farmaco 59 (2004) 615–625.
[25] A. Rosowsky, R.A. Forsch, S.F. Queener, J. Med. Chem. 45 (2002) 233–241.
[26] N. Agarwal, P. Srivastava, S.K. Raghuvanshi, D.N. Upadhyay, S. Sinha, P.K. Shukla, V.J. Ram, Bioorg. Med. Chem. 10 (2002) 869–873.
[27] J. Morgan, R. Haritakul, P.A. Keller, Bioorg. Med. Chem. Lett. 13 (2003) 1755–1757.
[28] V. Vanheusden, H. M-Lehmann, M. Froeyen, L. Dugue, A. Heyerick, D.D. Keukeleire, S. Pochet, R. Busson, P. Herdewijn, S.V. Calenbergh, J. Med. Chem. 46 (2003) 3811–3821.
[29] B. Desai, D. Sureja, Y. Naliapara, A. Shah, A. Saxena, Bioorg. Med. Chem. 4 (2001) 1993–1997.
[30] P.S. Kharkar, B. Desai, H. Gaveria, B. Varu, R. Loriya, Y. Naliapara, A. Shah, V.M. Kulkarni, J. Med. Chem. 45 (2002) 4858–4867.
[31] SYBYL 7.1, Tripos International, 1699 South Hanley Rd., St. Louis, Missouri, 63144, USA.
[32] E.J. Martin, J.M. Blaney, M.A. Siani, D.C. Spellmeyer, A.K. Wong, W.H. Moos, J. Med. Chem. 39 (1995) 1431–1436.
[33] Tripos Bookshelf 7.1, Tripos International, 1699 South Hanley Rd., St. Louis, Missouri, 63144, USA.
[34] S. Wei-Ke, Acta Crystallogr., Sect. E 62 (2006) 1431–1432.
[35] R.D. Cramer, D.E. Patterson, J.D. Bunce, J Am. Chem. Soc. 110 (1988) 5959–5967.
[36] G. Klebe, U. Abraham, T. Mietzner, J. Med. Chem. 37 (1994) 4130–4146.
[37] G. Klebe, Perspect. Drug Discov. Des. 12 (1998) 87–104.
[38] M. Böhm, J. Stürzebecher, G. Klebe, J. Med. Chem. 42 (1999) 458–477.
[39] S. Wold, E. Johansson, M. Cocchi, PLS—Partial Least Squares Projections to Latent Structures, in: H. Kubinyi (Ed.), 3D-QSAR in Drug Design; Theory Methods and Applications, ESCOM, Lieden, 1993, pp. 523–550.
[40] B.L. Bush, R.B. Nachbar, J. Comput. Aided Mol. Des. 7 (1993) 587–619.
[41] C. Legar, D.N. Politis, J.P. Romano, Technometrics 34 (1992) 378–399.
[42] L. Collins, S.G. Franzblau, Antimicrob. Agents Chemother. 41 (1997) 1004–1009.